# Fast Accurate Multi-Key Weight Measurement

Stefanie Gutschmidt[1] Mark McGuinness[2] William Munn[3]
James Hannam[4] Emma Greenbank[5] Soomin Jeon[6]
Chang-Ock Lee[7] Celia Kueh[8] Tony Gibb[9] Ben Goodger[10]
Andrew McIntyre[11]

January 27, 2018

**Abstract**

We consider an industrial problem brought to the Mathematics in Industry New Zealand (MINZ) study group in 2016, where items pass briefly over load cells resulting in a noisy oscillatory signal, from which the mass of the item is to be computed. We compare results obtained using a single load cell, with results from passing over two load cells in tandem or in succession. We develop mathematical models to assist with the computation of total load mass, considering both deterministic and statistical approaches.

## Contents

# 1 Introduction

Compac designs and exports equipment that sorts fruits and products for orchard packhouses. They presented a challenge to the 2016 Mathematics in Industry New Zealand (MINZ) study group, entitled *Estimating the Weight of a Moving Article Across Multiple Weigh Points*. Compac also presented challenges to MINZ and MISG (Mathematics in Industry Study Group) in previous years. For instance in the 2004 Compac Challenges were "The Boxing Problem" and "The Bagging Problem" [1]. The former challenge was about filling boxes with a specific number of articles to specifications such as minimum weight and maximising the number of boxes packed. The "Bagging Problem" was about filling bags above a minimum weight and maximising the number of bags packed, amongst other criteria. In 2015 Compac brought forward another challenge to MINZ, entitled "Calibration Transform for Discrete Spectroscopic, Mechanical and Optical Systems". This project aimed at creating a calibration transform that would convert the output of different spectroscopic systems to a standardized form. All these problems, including the Compac challenge of this work, the MINZ or MISG teams built mathematical and computational models to understand and predict the physical situation and to improve and optimize algorithms the processes. Proposed solutions by the study groups and teams have directly impacted and significantly improved Compac's boxing, weighing, bagging, and sorting software processes, which led to increased quality and productivity of their equipment and systems.

The work presented here is based on the results of the MINZ 2016 study group. Part of the fruit sorting process relies on fruit being weighed as it briefly passes over load cells (LC) on a conveyer belt. The fruit is supported by holders or keys. The weighing table needs to be able to deal with a range of fruit sizes and geometries. For instance, some fruit in the proposed new design will be supported by a single holder or *key* that will be measured as the single key moves over a load cell, and previous conveyor belt designs used a single holder for a single piece of fruit. The new design of the weighing section has led to the possibility of having one piece of fruit or any other article on multiple keys, to allow each key to remain on a load cell for a longer period of time than in previous single-holder designs. Now, articles may rest on one or multiple keys (Fig. 1), which are weighed sequentially, key-by-key. The main challenge arising from the proposed multi-key weighing machine is the measurement of the distributed weight of the article by multiple keys, typically with unknown contact points and locations, as in the case of the kumara[1] (c.f. Fig. 1b)). Inferring the weight of a piece of fruit on such a machine is complicated by the multiple support points, the fact that the article and/or the key may bounce during the weighing time, and the signal noise arising from the engineering environment. Compac are particularly interested in assessing whether the new design, with the help of some mathematical postprocessing of the data, is effective in improving the accuracy of the weighing process. Compac aims at an accuracy tolerance of smaller or equal 1 g for single-key and 5 g for multi-key articles.

In this paper we analyse and post-process data to find the most desirable weighing

[1]Sweet potato, called kūmara in New Zealand.

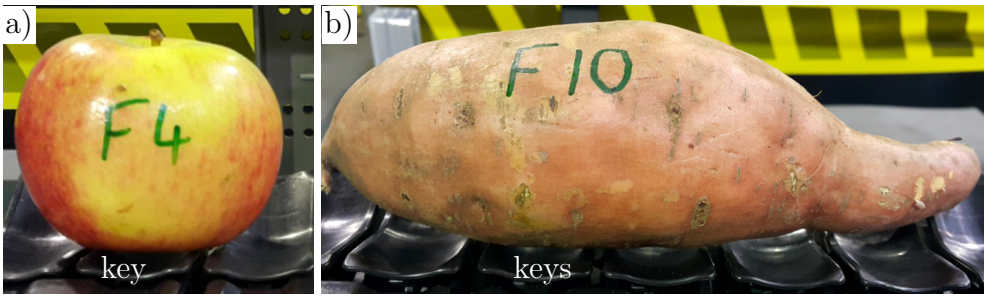


Figure 1: Articles on conveyor belt system. a) single-key article (apple); b) multi-key article (kumara).

solution for COMPAC's existing measuring system. The analysis will answer the following three key questions:

1. Currently, there are two measuring concepts (see Section 1.1) - parallel and serial - with which articles are measured. Which of the two measuring set ups - single or dual load cell - provide a higher accuracy?

2. Can a mathematical model be developed that is able to estimate the true weight of the article from recorded data sets for all considered articles single and multi-key alike?

3. What is the estimated theoretical weighing accuracy for a given conveyor belt velocity?

## 1.1 Single key versus multiple keys

The simultaneous two-key or parallel weighing method measures the weight on a pair of keys that simultaneously pass over two load cells, and outputs signals from each of the load cell. The data used in our analysis is from a seven key set up illustrated in Fig. 2. We refer to keys by consecutive number, with number 1 being the first key, and number seven being the last. The support points of the keys are organised such that three keys (namely keys 2-4-6) are measured on load cell one and four keys (namely keys 1-3-5-7) are measured on load cell two. In this set up the keys are weighed simultaneously in pairs, excluding key 7 which has no pair; key 1 is weighed on load cell two simultaneously with key 2 on load cell one, and so forth.

In contrast, in the single-key or serial weighing method the keys pass over one load cell sequentially and due to the design of the weigh beam the single-key measurements are made in half the period of time that is available when using the parallel weighing method. Data obtained with the single-key method are generated by another load cell (load cell three, with a wider top plate) that is impacted by all seven keys (not shown).

The data we considered during the study group was obtained for a setup with just seven keys in total, which go over the weigh-bridge with three load cells, crossing them as detailed above, then loop around and go over it again. Fruit or test weights are added by hand to the keys, before they reach the weigh-bridge, and are removed after the weigh-bridge before the keys loop around to begin again. The placement of fruit is repeated

several times in one data run. Hence the data shows at various times, load cells with nothing on them, or with empty keys moving across them, or with a loaded key moving across them. The mean signal value indicates which case obtains at any given time.

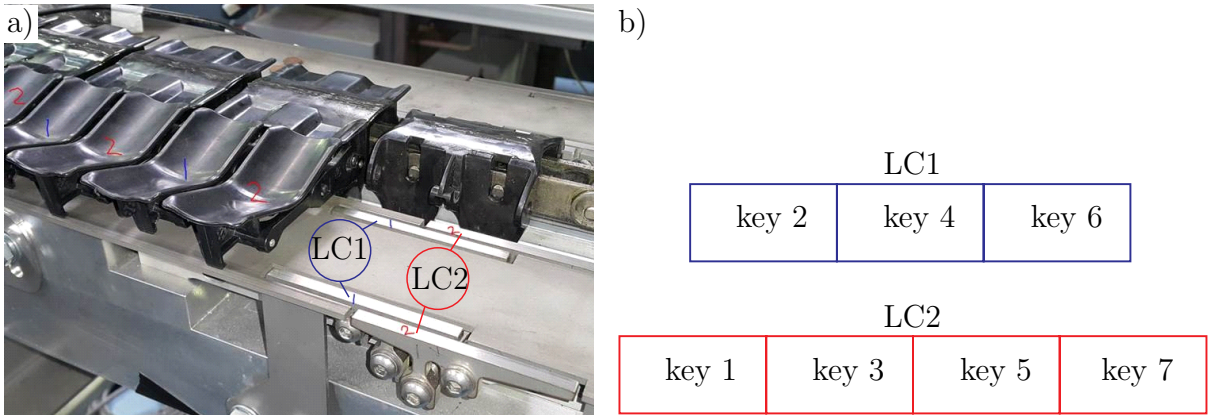


Figure 2: Key and load cell numbering system. a) Real system. b) Schematics.

Compac currently operates an automatic system that specialises in weighing fruits or articles based on single-key technology. The method estimates the weight of the article by calculating the average of the low-pass filtered output signal from the load cell for a time range when the key and fruit passed over the load cell (see Fig. 3; key 2 has the mandarin on it; the other keys are empty but they weigh about 18 g). An estimation of the weight of a single-key article such as e.g. the mandarin (Fig. 3) using this average technique is within 0.3 g of its actual weight at this belt speed.

When the simultaneous weighing method is applied to a two-key sized fruit (e.g. a pear) there are two potential outcomes based on the position of the article or fruit on the key(s). In the first case the fruit is positioned such that the fruit lies on a key pair with each key simultaneously supported on a separate load cell as illustrated by the signal in Fig. 4a. In case two the fruit is positioned such that the key pair is measured in a staggered manner, each key being weighed in separate time windows and thus its weight is recorded sequentially instead of simultaneously as illustrated in Fig. 4b.

The motion of the keys over the load cells (and other obstacles) cause the articles to arbitrarily separate from the keys and thus causing the fruitarticle to lift off. If the lift-off happens entirely on one key the full weight of the fruit is supported by the remaining key(s) for the lift-off duration. In this case the weight of a two-key article is estimated with the average method as a one-key article for the duration of the lift-off (see Fig. 4a). Applying this method the weight of the pear is estimated to be 165.11 g, where its actual weight is 165.26 g (error 0.1 %, or 0.15 g $<$ 1 g).

When a lift-off occurs such as in case two, the prior method cannot be used as this shifting weight can not be captured simultaneously on each load cell. Ignoring this and treating the data as if the fruit would be supported on one key, the prediction of the weight by adding partial weights from two keys together falls outside the acceptable error tolerance of 1 g. However, measuring the weight of the pear in a staggered manner (article is resting on keys 2 and 3, Fig. 4b), the predicted weight is 164.2 g which also lies outside of the desired error tolerance. The importance of considering the aforementioned

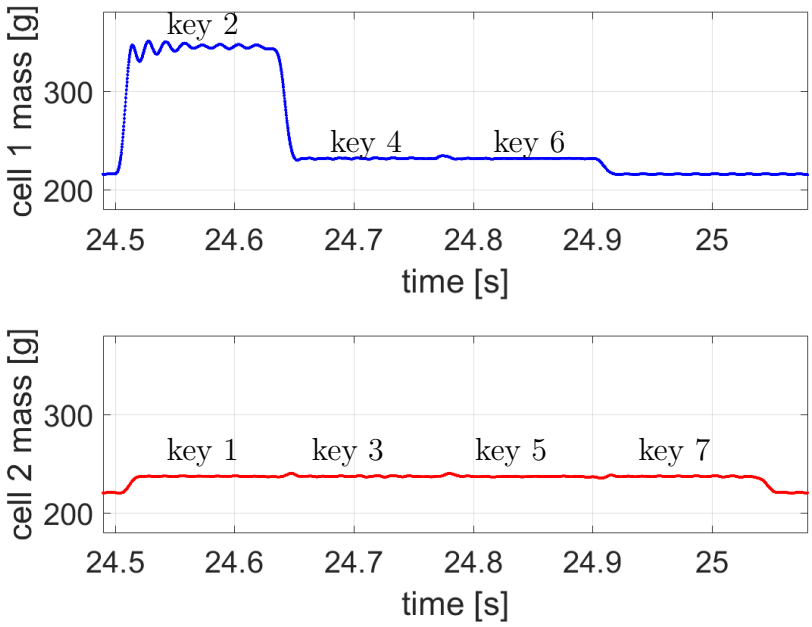


Figure 3: Filtered load cell signals for a mandarin sitting on a single key, belt speed 900 rpm. The zero weight is arbitrary at about 220 g for both cells. An empty key weight gives a mass change of about 18g; the mandarin a further 110 g approximately. Note that key 1 (load cell 2) is empty while passing over the load cell system together with the mandarin on key 2 (load cell 1) simultaneously (see Fig. 2).

measuring methods, simultaneous and staggered, becomes more obvious when considering an article that spans more than two keys (see Fig. 5); in such a case it is impossible for the entire article's weight to be measured simultaneously.

The load cell voltage signals are statically calibrated by four different calibration masses (ranging from 67.31 g to 200.03 g) as well as with empty keys (which have slightly differing weights about 16.31 g) and for all three load cells. The calibration curves are linear and the calibration factors are directly implemented in the analyses. Unless otherwise specified we directly present measured masses in gram and not in voltage.

Note that for an initial proof of concept of this method time ranges where eye-balled manually at values after and before jumps, respectively and according to the resolution of the data set. Compac Sorting monitors the speed of the belt per minute (RPM) and the length of the keys is known by design. Furthermore, optical sensors are used to record key to load cell interactions. Therefore, in an automated process the exact time ranges are readily available.

## 1.2 Data Analysis

The parallel set up (on two load cells) produces two simultaneous signals. In the data provided by Compac, as detailed above, a total of seven keys pass over the two load cells. The single load-cell method (# 3) produces one signal from 7 keys in succession. As above, in this section we use only the low-pass filtered signals that is provided directly

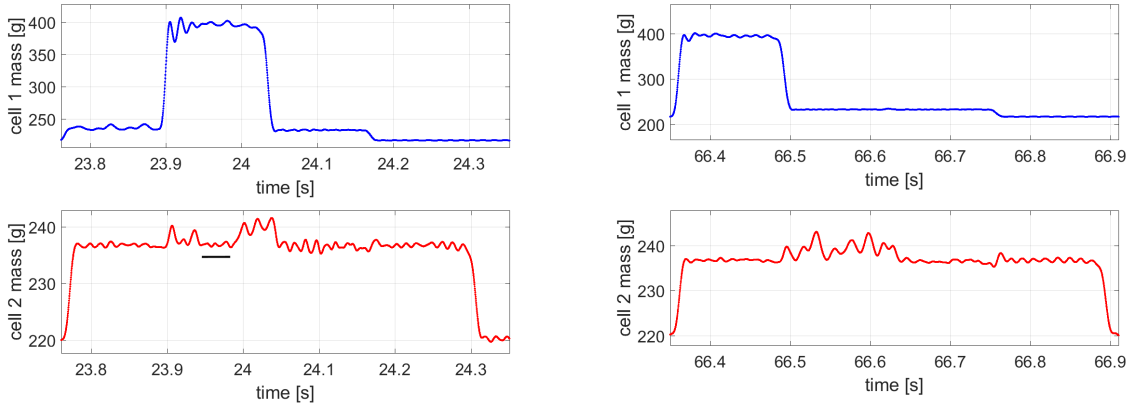


(a) Simultaneous weight measure. The pear is mainly carried on key 4, but some of its weight is also on key 3, both measured during the same time range $(23.9, 24.05)$ s. Lift-off of the fruit from the key is observed in the signal behaviour indicated by the black line.

(b) Staggered weight measure. The pear is mainly on key 2, weighed during the time period $(66.3, 66.5)$ s, but apparently some part is bouncing onto key 3 during the next measuring period.

Figure 4: Load cell signals for a pear positioned on two keys, belt speed 900 rpm.

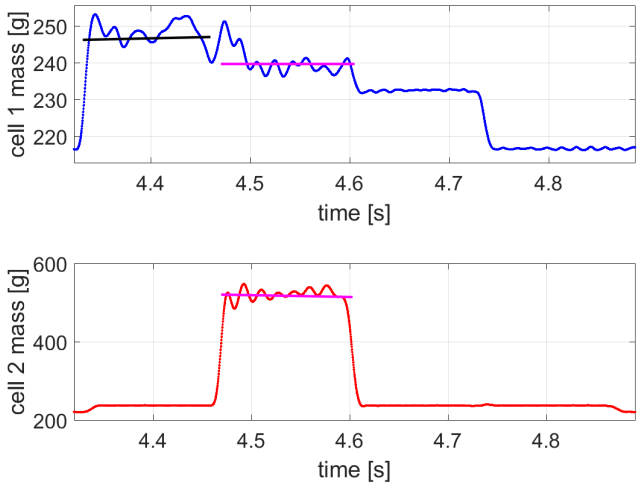


Figure 5: Kumara weighing data, belt speed 900 rpm.

from the load cells.

Compac currently operates equipment that weighs single-key fruit successfully. Their current method involves taking the average of the filtered signal from a load cell after initial transients have subsided. This method provides an estimated weight with under 1 g of error, for fruit that is not too heavy and for moderate belt speeds.

As discussed above, when weighing a multi-key article, there are two possible scenarios for the article to pass over the load cells, namely simultaneously or successively. These cases will result in qualitatively dissimilar signals, as the dynamic behaviour of keys dropping on to a load cell may cause fruit to move or even to bounce off of a key for a

time instant. At the moment of lift-off for scenario one, the article's entire weight might be assumed to be supported by the remaining key, from which a very accurate measurement can be obtained by using COMPAC's single-key method. Should a lift-off occur for case two (successive measurement), however, the single-key method fails. Another degree of complexity is added by fruit bouncing between two or more keys due to the dynamic nature of the motion, which introduces transient signals due to impact and rebound and thus altering the apparent weight of the fruit.

Considering a multi-key article such as the kumara from the previous section again (Fig. 5), there are two ways of using an averaging technique to approximate the weight of a multi-key article. In each case, we take the average value of the signal $f(t)$ over some time window $\Delta t$ starting from time $t_0$. By first adding the signals of the load cells together, and then taking an average of the combined signal we can gain an estimate for the weight of the article on each key pair and identify any simultaneously recorded dynamics. The total weight of the article is then estimated by adding up the estimates for each key pair. We will refer to this method as the *combined signal* method. Alternatively, we can first split the load cell signals up into separate key signals and take an average of the individual signals. Calculating the sum of the averages of all key signals provides an estimate of the total weight of the fruit. This method is referred to as the *separate signal* method. Note, that for the single-cell load cell measurement method (# three as described in Section 1.1 on p. 3), the latter method for finding weight estimate must be used.

Testing these methods on a potato they were found to provide practically identical estimates, which, however, fall outside of the desired error tolerance of 1 g (Fig. 6). The

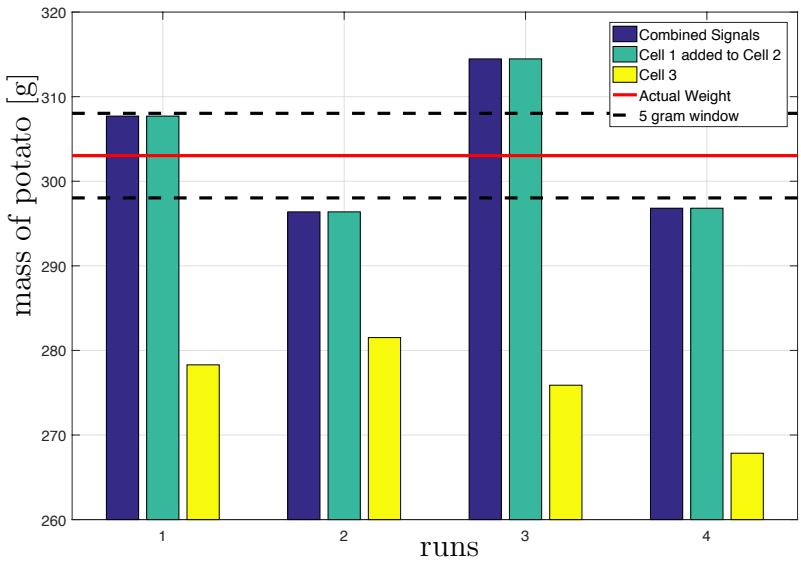


Figure 6: Potato weights calculated using different weighing methods.

combined signal method and the separate signal method both produce better results from the parallel load-cell data than predictions estimated from the single load-cell data (Fig. 6). This reveals a conclusion and answer to the first question of Section 1 about the accuracy between parallel and serial load-cell measurement methods. The parallel load-cell set up provides higher accuracy measure than the single load-cell set up.

## 2 A Geometric Approach

In this section we consider a slightly different (geometric) approach to extract the weight from a raw load-cell signal that is oscillating due to damped harmonic motion. This approach largely follows that of Kesilmis and Baran [2]. We have modestly extended their findings in the following three main ways:

1. by developing an explicit formula for the static equilibrium voltage;
2. by demonstrating the both linear and nonlinear interpolations give rise to the same solution for the static equilibrium voltage; and
3. by comparing these results with those obtained with a computer program that solves this problem using iterative methods.

The static equilibrium of a dynamic system is the mean value about which the object oscillates when in motion. For this highly dynamic weighing process of articles the mean value needs to be extracted from the signal. This off-set value is subject to change for every key and key-article combination.

The motivation for a geometric approach is as follows: the weight force that an article applies to the keys (and hence the load cell) typically causes the load cell to produce a voltage/time signal that resembles damped oscillations. Determining the equilibrium from the signal amounts to knowing the combined mass of the article of fruit, and the keys over which it spans (since the mass of an object on the load cell is linearly related to the voltage that the load cell outputs). Once this combined mass value is known, the masses of the keys (approximately 16 g each) can be subtracted, leaving the mass of the fruit, which is, of course, what COMPAC is interested in knowing.

To the extent that the voltage signals produced by the load cell can be modelled by damped sinusoids, we can exploit geometric properties of sinusoids to determine this off-set voltage. In the following we outline this method by referring to the details of Fig. 7, which illustrates how this method is applied to a typical set of damped oscillations.

1. Locate three adjacent *local extrema* in the signal, with coordinates given by $(t_1, v_1)$, $(t_2, v_2)$, $(t_3, v_3)$, where $v_i = v(t_i)$ for a voltage/time signal $v$.
2. Interpolate between $t_1$ and $t_2$ with a function $v_I(t)$, and again between $t_2$ and $t_3$ with a function $v_{II}(t)$ (using either straight lines, or trigonometric functions).
3. Determine the special time, $T^*$, for which $v_I(T^*) = v_{II}(T^* + \Delta t)$ with $\Delta t = t_3 - t_2 = t_2 - t_1$ being the half-period of the oscillation.
4. Determine the off-set voltage, $v^*$, by evaluating $v_I(T^*)$.

The key for solving for both $T^*$ and $v^*$ is the assumption that the time intervals between the occurrence of each pair of local extrema is constant. In reality some variations would be present, but expected to be sufficiently small and therefore treated as negligible.

We now give a brief derivation of both linear and nonlinear "interpolation" functions. Figure 7 illustrates how we might go about doing so with straight lines. For instance, the

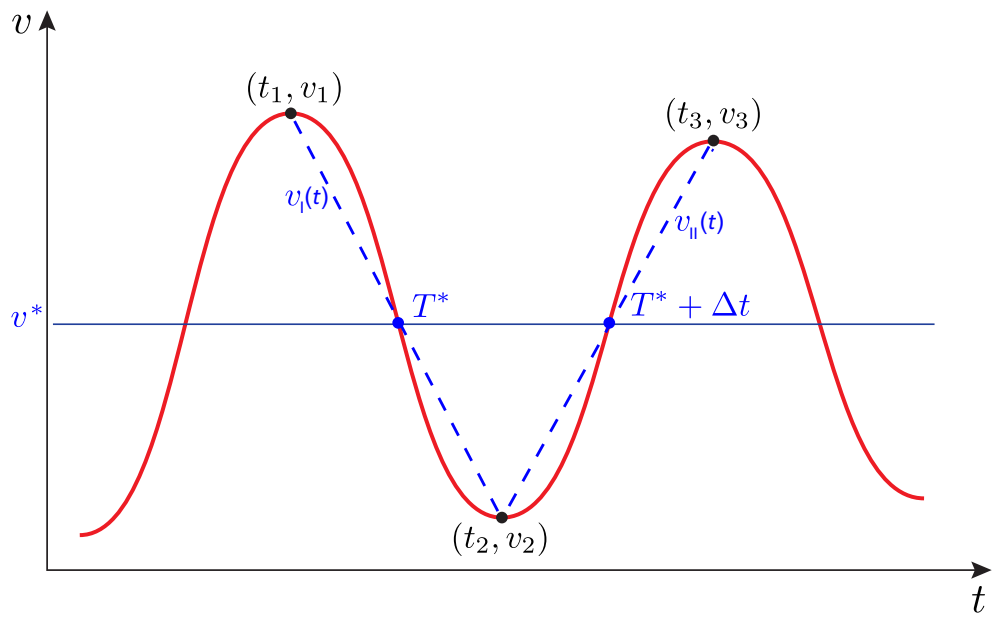


Figure 7: Linear interpolations to determine the off-set voltage.

straight line joining $(t_1, v_1)$ and $(t_2, v_2)$ has a gradient of $v_2 - v_1/t_2 - t_1$. It is described by

$$v_I(t) = \left(\frac{v_2 - v_1}{t_2 - t_1}\right) t + \frac{v_1 t_2 - v_2 t_1}{t_2 - t_1} \quad \text{for} \quad t_1 \leq t \leq t_2.$$

Similarly, the straight line that subsequently joins $(t_2, v_2)$ and $(t_3, v_3)$ is given by

$$v_{II}(t) = \left(\frac{v_3 - v_2}{t_3 - t_2}\right) t + \frac{v_2 t_3 - v_3 t_2}{t_3 - t_2} \quad \text{for} \quad t_2 \leq t \leq t_3.$$

These results agree with those in [2]. Imposing the geometric condition that

$$v_I(T^*) = v_{II}(T^* + \Delta t)$$

and recalling that $\Delta t = t_3 - t_2 = t_2 - t_1$ gives the result that

$$T^* = \frac{v_3 t_3 - 2v_3 t_2 + v_2 t_2 + v_2 t_1 - v_1 t_2}{2v_2 - v_1 - v_3}.$$

It can immediately be shown that the off-set voltage, $v^*$, is given by

$$v^* = \frac{v_1 v_3 - v_2^2}{v_1 + v_3 - 2v_2}.$$

In order to see that this formula makes intuitive sense, consider the case of totally *un-damped* motion. This has the consequences that $v_1 = v_3$. Therefore, replacing $v_3$ with $v_1$ in the expression for $v^*$ yields

$$v^* = \frac{v_1^2 - v_2^2}{2v_1 - 2v_2} = \frac{(v_1 + v_2)(v_1 - v_2)}{2(v_1 - v_2)} = \frac{v_1 + v_2}{2}.$$

This demonstrates that $v^*$ will return the correct value of the mean of the two local extrema $v_1$ and $v_2$, which represent a peak and a trough (in no particular order).

This formula for the off-set voltage can be derived in a slightly different manner. Instead of formulating *linear* interpolation functions $v_I$ and $v_{II}$, we can interpolate using portions of e.g. cosine functions. This is perhaps a slightly more intuitive approach, since we have assumed that the signals oscillate like sinusoids. The relevant interpolation functions in this case are:

$$v_I(t) = \frac{v_1 - v_2}{2} \cos\left(\pi\left[\frac{t}{\Delta t} - \frac{1}{2\Delta t}(t_1 + t_2) + \frac{1}{2}\right]\right) + \frac{v_1 + v_2}{2} \quad \text{for} \quad t_1 \leq t \leq t_2$$

and

$$v_{II}(t) = \frac{v_2 - v_3}{2} \cos\left(\pi\left[\frac{t}{\Delta t} - \frac{1}{2\Delta t}(t_2 + t_3) + \frac{1}{2}\right]\right) + \frac{v_2 + v_3}{2} \quad \text{for} \quad t_2 \leq t \leq t_3.$$

When we impose that $v_I(T^*) = v_{II}(T^* + \Delta t)$, we get the following solution for $T^*$:

$$T^* = \frac{1}{2}(t_1 + t_2) + \frac{\Delta t}{\pi} \cos^{-1}\left(\frac{v_3 - v_1}{v_1 - 2v_2 + v_3}\right) - \frac{\Delta t}{2}.$$

Assuming once again that $\Delta t = t_3 - t_2 = t_2 - t_1$, we can easily produce the same expression for $v^*$ as we did with the previous linear approach.

## 2.1 Results

The success of the formula we have derived for the off-set voltage, $v^*$, depends on the extent to which the actual voltage/time signals resemble damped simple harmonic motion. In many cases (especially where articles are irregularly shaped, and appears to rock among keys) the signals display considerable volatility. In these situations, the value for $v^*$ that the formula returns is also rather volatile.

An additional shortcoming of the expression for $v^*$ is that it assumes that the time between each local extrema is constant which might not be true in every case in the data. As a result, we have developed a computational method[2] (not presented here) for solving the problem in a more rigorous manner. This method does not use interpolation functions, but operates on the data itself. It finds the particular time, $T^*$, for which

$$v_I(T^*) = v_{II}(T^* + \Delta t)$$

where $\Delta t$ corresponds to the "mean half-period" of the particular set of three local extrema. (The raw data is discretised at intervals of $2.5 \times 10^{-4}$ seconds, which slightly constrains the accuracy of both methods.) Clearly, at no point does this assume (or require) that $t_3 - t_2 = t_2 - t_1$. In Figures 8a-8d below, we contrast the results of applying both the expression, and the computational method, to the signals of two man-made articles (A1 and A4), and also two real articles (F3 (Orange, 290.0 g) and F8 (potato, 74.7 g)).

There are several key observations that can be made from Fig. 8. The first is that both methods clearly return similar values - A1's estimated mass: 75.85 g (formula), 75.38

[2]The details of this program are available upon request.

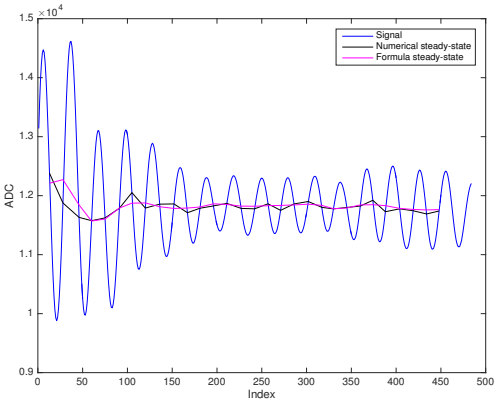


(a) Geometric approach applied to article A1.

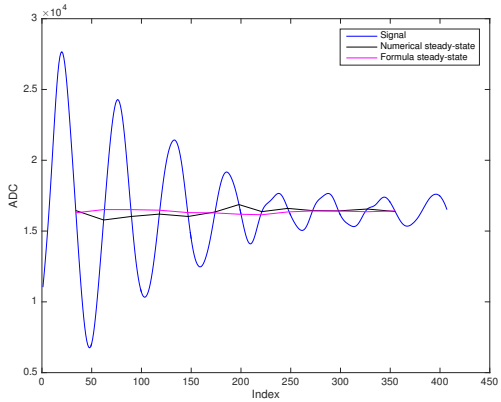


(b) Geometric approach applied to article A4.

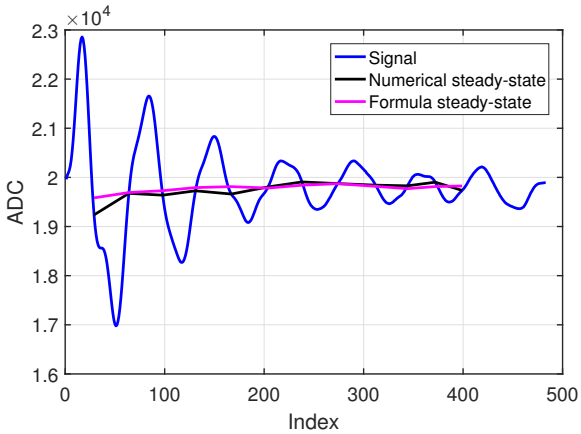


(c) Geometric approach applied to article F3.

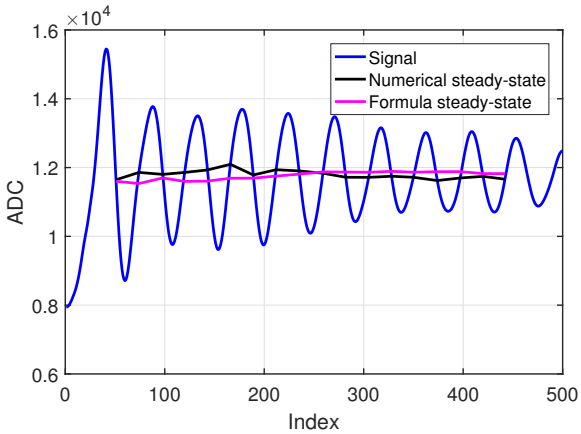


(d) Geometric approach applied to article F8.

Figure 8: Examples of applying the geometric method to filtered raw signals from load-cell data.

g (numeric method) and A4's estimated mass: 188.99 g (formula), 188.59 g (numeric), F3's estimated mass: 272.6 g (formula), 271.6 g (numeric method) and F8's estimated mass: 72.4 g (formula), 73.1 g (numeric method). However, these results fall outside the acceptable tolerance of 5 g (for multi-key articles), as e.g. the true masses of articles A1 and A4 were 80.8 g and 200.1 g, respectively. The second is that the formula we have derived for $v^*$, even though it assumes incorrectly that the "half-periods" between successive local extrema are equally spaced, seems to return a less fluctuated value for the off-set voltage, which is useful as these different values of $v^*$ would need to be averaged in order to produce a single voltage for a given article (and, therefore, a single mass). Indeed, the expression for $v^*$ often seems to smooth the volatility of the numerical solution; this is especially apparent in the case of article A1.

Overall, a geometric approach seems to hold some promise in solving the problem of high-speed weighing. In the case of an article that spans multiple keys, where there is sudden and unpredictable rocking or bouncing on keys, the signal may be sufficiently volatile that a geometric approach needs to be combined with another method. The application of these methods to signals where the article is known to rock or bounce should be the subject of further research in this area.

# 3 Nonlinear Fitted Solution Approach

In this section we consider an alternative and more sophisticated approach to those presented in previous sections, this time working directly with the raw (unfiltered) signal from any single load-cell as shown in Figure 9. The measure ADC (analogue to digital converted) signal is the converted voltage signal from the load cell.

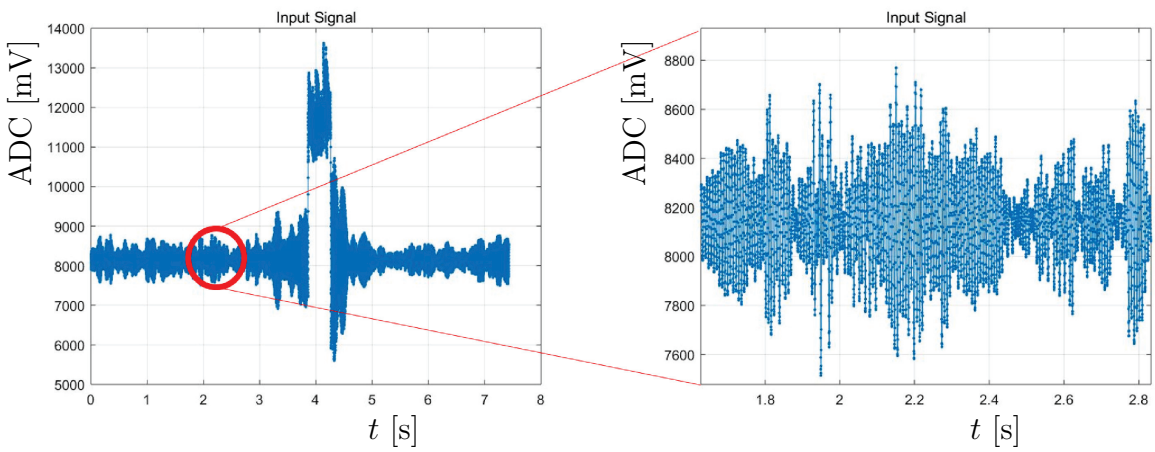


Figure 9: Unfiltered input signal.

We observe that the signal consists of two major components: one is a step function and the other is highly oscillatory. The former originates from the change of weight sensed by load cell. Even empty keys show a small abrupt change do to the change of sensed weight. For keys with articles on this jump is significant and easy to identify. The highly oscillatory nature of the signal has several technological origins, which are hard to tell apart due to their highly-likely coupling possibility. The underlying cause of the

dominating vibration, however, is initiated by the keys mechanically contacting the load cell (on/off).

We seek to use nonlinear optimisation to fit the signal simultaneously with a step function and a damped harmonic motion solution. For simplicity of presentation, we consider only one load-cell signal in this section, and the focus is on an effective method for rapidly filtering out the oscillations in the signal.

## 3.1 Mathematical modelling

Looking at Figure 9, we think of the signal $y$ from a load cell as being composed of a static component $y_s$ and a dynamic component $y_d$ from the raw signal $y_0$. It can be expressed as

$$y(t) = y_s(t) + y_d(t). \tag{1}$$

It is envisaged that the dynamic component $y_d$ might be separated from the static component $y_s$, which would be used for the determination of weight. To obtain the dynamic component of the signal $y_d$, we assume that it can be described as damped free vibration. Then, the dynamic component of the signal $y_d$ satisfies the equilibrium equation of forces for damped free vibration or simple harmonic motion. The damped free vibration of the system is given by

$$m\ddot{y}_d + b\dot{y}_d + ky_d = 0, \tag{2}$$

where $m$ is the total effective oscillating mass, $b$ is the damping coefficient, and $k$ is the effective spring constant of the load cell system.

Rewriting the equilibrium equation (2) after dividing by $m$, we have

$$\ddot{y}_d + B\dot{y}_d + Ky_d = 0, \tag{3}$$

where $B = \frac{b}{m}$ and $K = \frac{k}{m}$. The general solution to (3) may be written in the form

$$y_d(t) = A\,\mathrm{e}^{-\frac{Bt}{2}}\cos(\Omega t + \varphi), \tag{4}$$

where $A$ is the initial amplitude of the oscillation, $B$ is the damping coefficient relative to system mass, $\Omega$ is the natural frequency of the system (rad/s), and $\varphi$ is the phase shift (rad).

Now, we consider how to find the parameters $A$, $B$, $\Omega$, and $\varphi$ of the dynamic component $y_d$ and the static component $y_s$ which provide the best fit to the given raw signal data $y_0$. Since a new damped oscillation is generated each time a carrier key passes over a load cell as shown in Figure 9, there are big jumps in the values of signals at these points. Therefore, we consider piecewise processing of the load signal over a time interval for fitting the data.

## 3.2 Moving window processing

Consider a $k$-th time window $T_k$ centered on the time value $t_{k,c}$ as shown in Fig. 10. Each window covers $2n+1$ samples of data and consecutive windows overlap by $n$ data points. To reconstruct the signal on each window, we use $2n+1$ samples on each window

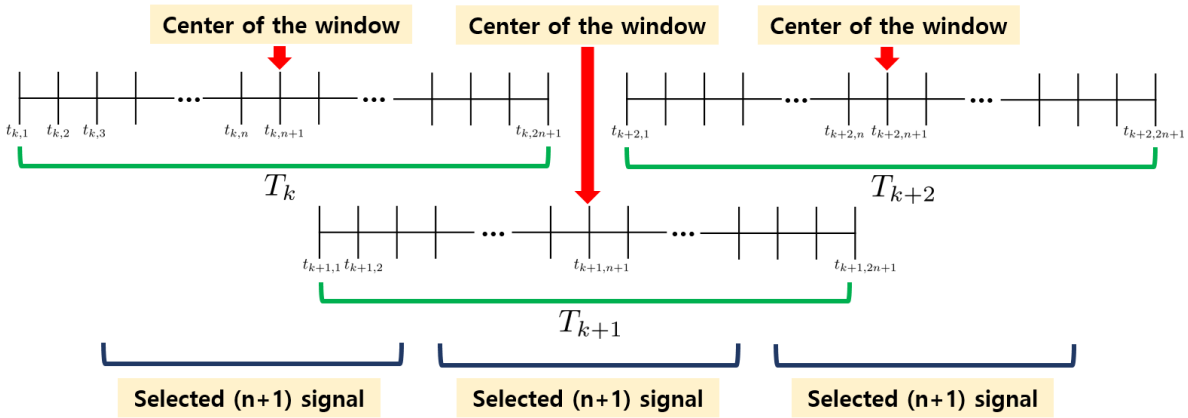


Figure 10: Description of the moving windows.

for fitting to, and we choose the middle $n+1$ values from the resulting fitted signal for reconstruction. Let $t_{k,a}$ and $t_{k,b}$ be lower and upper bounds of the time window $T_k$, respectively, then

$$t_{k,a} = t_{k,1} \leq t_{k,2} \leq \cdots \leq t_{k,c} = t_{k,n+1} \leq \cdots \leq t_{k,2n+1} = t_{k,b}.$$

Now, we have a nonlinear least squares problem over each time window $T_k$ and the least squares error $S_k$ over the time window $T_k$ is expressed as follows:

$$S_k(A, B, \Omega, \varphi, y_s) = \sum_{i=1}^{2n+1} |y(t_{k,i}) - y_0(t_{k,i})|^2. \tag{5}$$

We call the piecewise processing of the load signal the moving window process (Fig. 11).

## 3.3 Nonlinear data fitting

We apply the Levenberg-Marquardt algorithm [3, 4] for solving the nonlinear least squares minimization problem on each window. For the Levenberg-Marquardt algorithm, getting an initial guess that is close enough to the desired minimising value is crucial for convergence to the global minimum.

### 3.3.1 Estimation of the static component

For the static component $y_s$, we adopt the average value of the raw signal over $k$-th time window $T_k$ as an initial value. On each window $T_k$, an initial value is estimated as

$$y_s(T_k) = \text{average}\{y_0(t_{k,1}), y_0(t_{k,2}), \cdots, y_0(t_{k,2n+1})\}.$$

### 3.3.2 Estimation of the dynamic component parameters

The dynamic component of the signal $y_d(T_k)$ is obtained by subtracting $y_s(T_k)$ from $y_0(T_k)$. To find the dynamic component parameters using the Levenberg-Marquardt algorithm, we need to start with a good estimate of the initial value of each parameter.

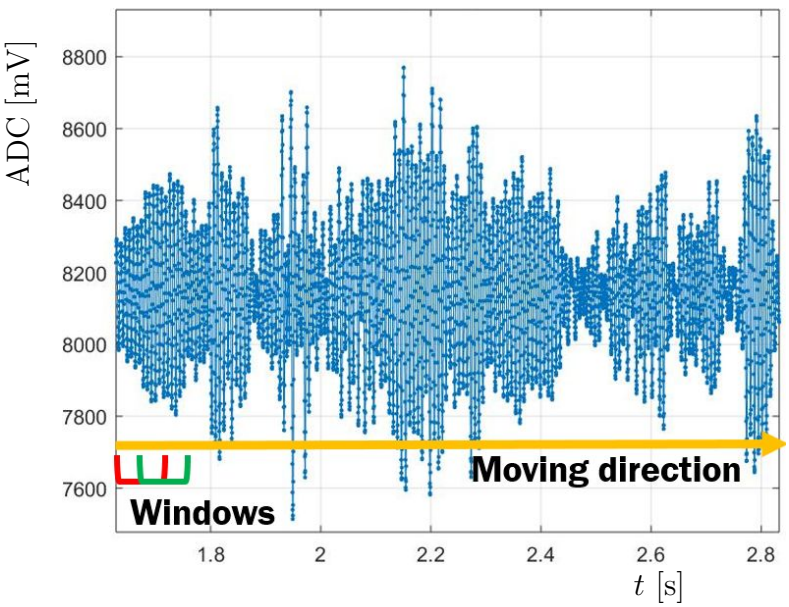


Figure 11: Description of moving window process.

Numerical differentiation with respect to time is performed to obtain estimates of $\dot{y}_d$ and $\ddot{y}_d$ on $T_k$. A system of equations based on (3) can be written for each time in the time window $T_k$:

$$\begin{bmatrix} y_d(t_{k,a}) & \dot{y}_d(t_{k,a}) & \ddot{y}_d(t_{k,a}) \\ \vdots & \vdots & \vdots \\ y_d(t_{k,b}) & \dot{y}_d(t_{k,b}) & \ddot{y}_d(t_{k,b}) \end{bmatrix} \begin{bmatrix} K \\ B \\ 1 \end{bmatrix} = \begin{bmatrix} 0 \\ \vdots \\ 0 \end{bmatrix}. \tag{6}$$

The linear system (6) can be rewritten as

$$M \begin{bmatrix} K \\ B \end{bmatrix} = \mathbf{f}, \tag{7}$$

where $M$ is an $(2n+1) \times 2$ matrix and $\mathbf{f} \in \mathbb{R}^{2n+1}$. We then find initial estimates of $K$ and $B$ by solving the $2 \times 2$ normal equation

$$M^T M \begin{bmatrix} K \\ B \end{bmatrix} = M^T \mathbf{f}.$$

An estimate of parameter $A$ is found from the maximum of $y_0 - y_s$ within the time window $T_k$ as

$$A = \max_{t_{k,i} \in T_k} |y_0(t_{k,i}) - y_s(t_{k,i})|.$$

The estimate of $\Omega$ is given by

$$\Omega = \sqrt{K - \left(\frac{B}{2}\right)^2}.$$

The phase shift $\varphi$ is estimated as

$$\varphi = \cos^{-1}\left(\frac{y_d(t_{k,a})}{A}\right).$$

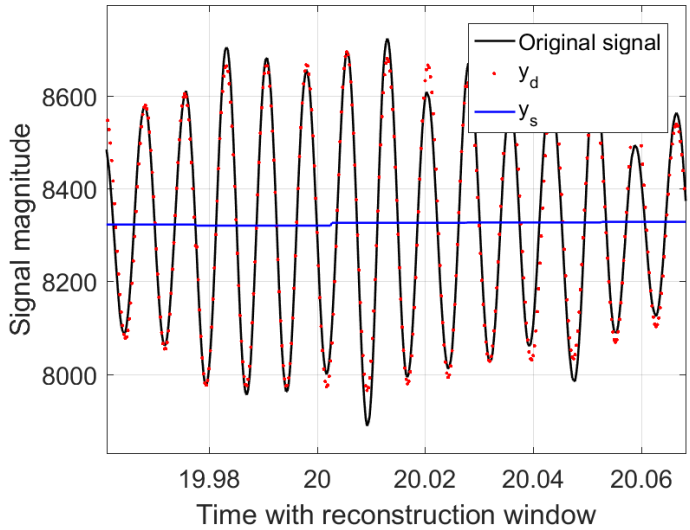


Figure 12: Result of the deterministic approach, after fitting simple harmonic motion (red symbols) to raw data (black curve). The fitted step values approximating the mass, which can be regarded as a filtered signal, can also be seen (horizontal blue lines), for three windows.

Using the above estimates as an initial guess, we solve the minimization problem (5) to reproduce the signal $y(T_k)$ by the Levenberg-Marquardt algorithm. The reproduced signal $y(T_k)$ is shown in Figure 12, during a time when there is no key on the cell. The fitted step values are relatively close to each other, indicating a reasonably stable filtered signal value for the zero additional load case.

## 3.4 Results

We applied our algorithm to the data set `a9-900rpm` to illustrate the performance of the proposed approach. Article F9 is a red potato with a measured weight of 303.03 g. As shown in Figure 13, the signal is highly oscillatory even when empty carrier keys are passing over the load cells.

Relatively high-valued peaks occur when a carrier key supporting an object is on a load cell. There are three peaks visible in the given data and we indicate them using the numbered red arrows in Figure 13. The signals of the corresponding time intervals are shown in more detail in Figure 14. To fit the signal in `a9-900rpm`, we used a window size 101 and the size of the intersection between consecutive windows was 50 sampled points. Since the signal data in `a9-900rpm` is sampled every 0.25 ms, each window covers a time interval of about 25 ms.

Figure 15 shows the graph of the reproduced signal obtained by using our approach. The zoom-in graphs of the reconstructed signal on the time intervals 12.60∼13.00 ms, 24.58∼24.98 ms, 45.90∼46.30 ms, and 67.21∼67.61 ms are given in Figs. 16a to 16d, respectively. The black line indicates the original input signal, the red dots are the points on the reproduced signal, and the blue line shows the static component $y_s$ obtained on each window.

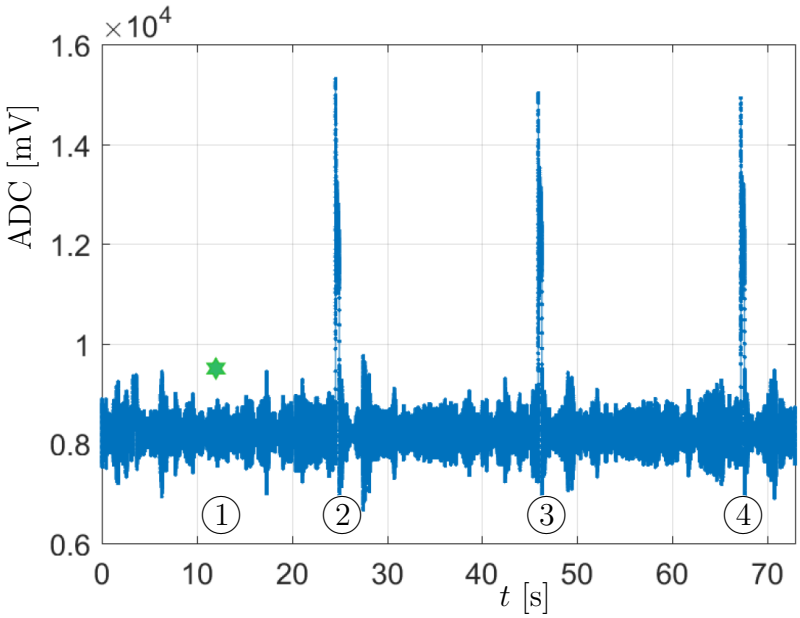

Figure 13: The load cell data obtained using item A9 travelling at 900 rpm, showing the four intervals chosen for analysis. Note, that the one labelled with a star has nothing on the keys, and the other three are when item A9 is on the keys crossing the load cells.

Table 1 shows information of the static component of the reproduced signal on each windows covering the time intervals 12.60∼13.00 ms, 24.58∼24.98 ms, 45.90∼46.30 ms, and 67.21∼67.61 ms.

The a9-900rpm as well as other data sets that have been used for our algorithms and analyses are proprietary to Compac Sorting Equipment Ltd.

# 4 Statistical Approach

Thematically, we have thought about gaining as much prior information about the individual articles as possible before they hit the load cells. This is made possible through the vision technology that Compac implement. Compac currently use a camera to take photos of an article moving at high speed. This image can be processed rapidly in order to determine characteristics such as the diameter, and any external deficiencies such as discolouration that might be present. This complements the actual weighing process in informing packers as comprehensively as possible. We have posited two specific approaches to using this prior information. A simple top down photograph of an article of fruit is sufficient to generate a crude approximation to the mass of that article. For example, it is a simple task computationally to fit an ellipse to the outline of a piece of fruit, from which we could interpolate a three dimensional envelope of an ellipsoid, say, and then use an approximate value for the density of the article to estimate its mass. A typical density range across different types of fruit are $10^2 - 10^3$ kg/m$^3$.

Even the fairly crude approximation of the mass that this process would produce would be useful, for example as an initial estimate of mass in a parameter-fitting approach like the Levenberg-Marquardt method discussed in the previous section. At the

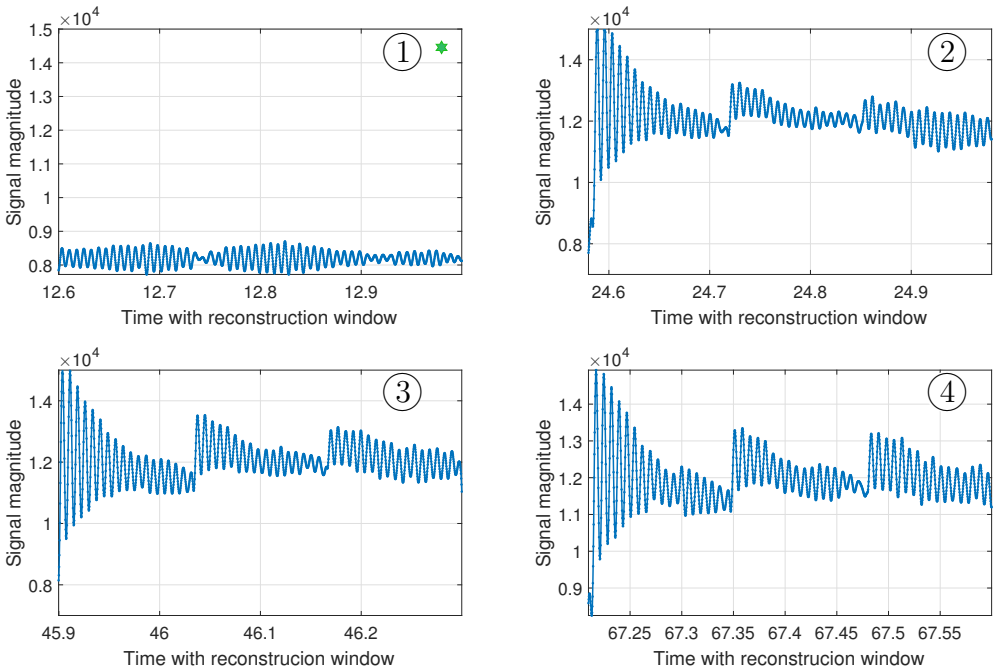


Figure 14: Expanded views of the four time intervals chosen to analyse item A9 at 900 rpm, as shown in Fig. 13. The first interval, labelled with a star, shows the baseline signal when keys are empty.

moment, the signals that the load cells are producing are essentially the sum of an idealised step function, representing the true mass of the article being weighed, as well as noisy oscillations, caused by the natural oscillatory motion of the article as it bounces and rocks on the keys and load cells. Using the approximate mass value, a physical model can produce such a simple harmonic signal, which can then be backed out of the noisy signal, which will give us a better estimate of the true mass of the article.

Our second approach does not assume an accurate physical model for the motion of the article. Instead, it is based around searching a data base of averaged signals, accumulated over time, each average corresponding to a specific kind of an article and a specific combination of keys on which it rests. Prior knowledge, before the load cell measurement, includes the type of the article, the estimated weight, the number of keys that are being spanned (but not necessarily touched) by the article and the chain speed. This information defines an expectation space in the data space of averaged signals in our library. If the current load cell output is cross-correlated to all entries in the expectation space, one result will produce a higher correlation than others. The averaged signal that best correlates with the current signal allows the weight of the fruitarticle to be read out from the data base.

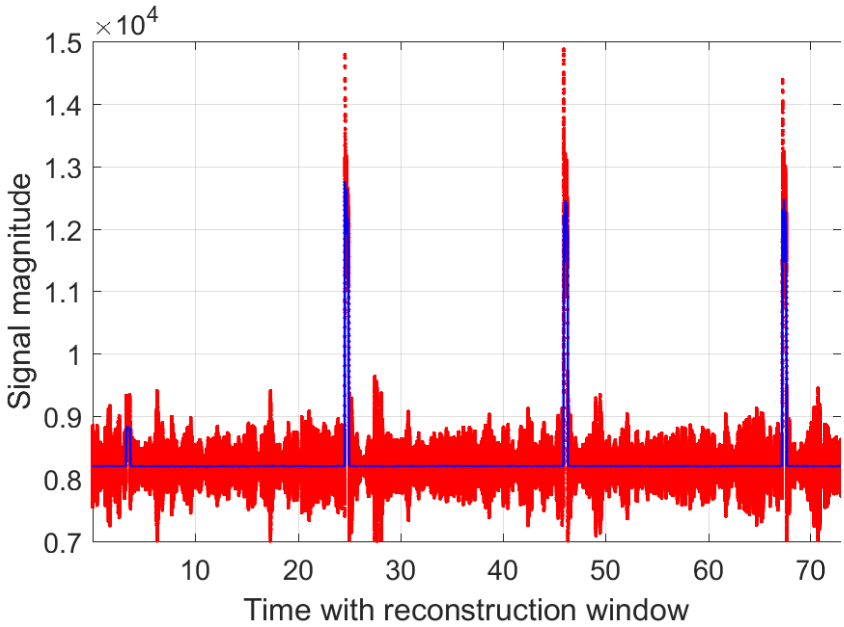


Figure 15: Data (black curve), fitted signal $y_d$ (red symbols), and fitted step functions $y_s$ (horizontal lines) for the full data set. Three loaded key events are clearly visible during this time period. The filtering performed in getting the step functions also clearly identifies the empty keys passing over the weigh table near $t = 3$ s early in the time series.

# 5 Summary and Conclusion

We have addressed the challenge of weighing articles on multiple support keys in a variety of ways. In summary the three questions posted in Section 1 are answered as follows:

**1) Currently, there are two measuring concepts - parallel and serial - with which articles are measured. Which of the two measuring set ups - single or dual load cell - provide a higher accuracy?**

We found that the doubling of time on the load cell that is consequent upon using staggered keys does improve weighing accuracy over the conventional single holder system used by Compac, when considering the low-pass filtered signal provided by the load cells (c.f. Section 1.2). The low-pass filter is too slow for the single holder at this conveyor belt speed, leading to a consistent under-estimation of the fruit weight for the single holder, as evidenced in Figure 6.

**2) Can a mathematical model be developed that is able to estimate the true weight of the article from recorded data sets for all considered articles single and multi-key alike?**

When the considered article is supported by more than one key, a static approach reveals that the weights recorded for each key should be added together. We found there was no detectable difference in accuracy, between adding the filtered signals before computing mass, and adding the computed masses from the separate filtered signals, as in Figure 6.

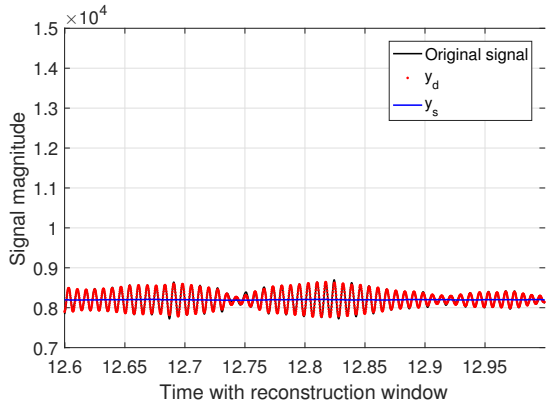


(a) Data (black curve), fitted signal $y_d$ (red symbols), and fitted step functions $y_s$ (horizontal lines) expanded for the star event, with no load on the keys (24.58∼24.98 ms)

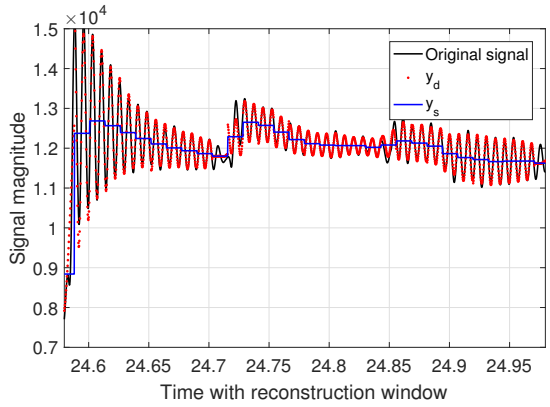


(b) Data (black curve), fitted signal $y_d$ (red symbols), and fitted step functions $y_s$ (horizontal lines) expanded for the first event with keys loaded (24.58∼24.98 ms)

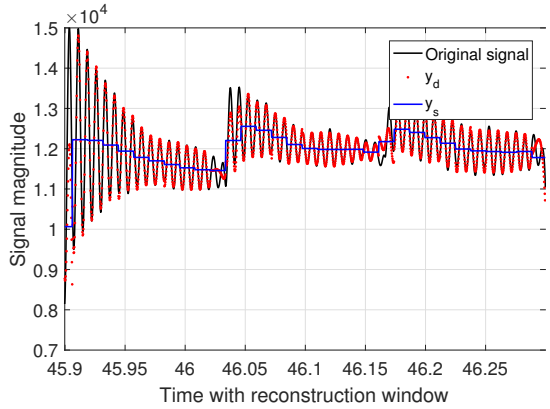


(c) Data (black curve), fitted signal $y_d$ (red symbols), and fitted step functions $y_s$ (horizontal lines) expanded for the second event with keys loaded (45.9∼46.3 ms)

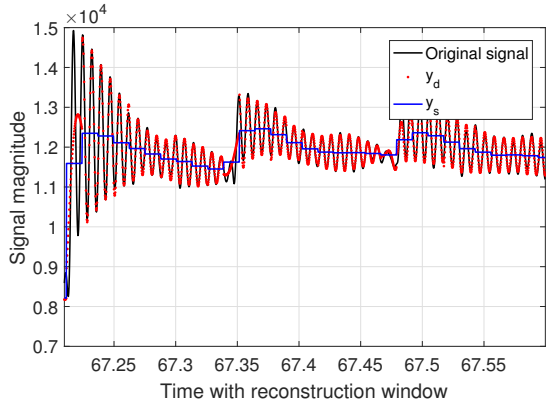


(d) Data (black curve), fitted signal $y_d$ (red symbols), and fitted step functions $y_s$ (horizontal lines) expanded for the third event with keys loaded (67.21∼67.61 ms)

Figure 16: Results of fitting simple harmonic motion plus a step function on moving windows to the raw data from a load-cell.

However, if random noise is affecting the signal then in principle we expect that adding raw signals before processing is better, as adding can lead to a partial noise cancellation effect.

We see some evidence (Figure 4a) that articles supported by more than one key are sometimes rocking or bouncing off one key, which reduces the accuracy with which the mass might be estimated from the load-cell signal. It may be useful to try to model the nonlinear dynamics of bouncing and rocking, to identify when it may be occurring and possibly to indicate how to modify the signal processing required to obtain improved mass estimates during bouncing or rocking.

We consider the developed mathematical models very suitable for measuring single and multi-key articles. We, however, suggest that a technological solution is found to

Table 1: The static component of the reproduced signal on each window

| Time interval (scale of $y_s$) | 12.60∼13.00 ms ( $\times 10^3$) | 24.58∼24.98 ms ( $\times 10^4$) | 45.90∼46.30 ms ( $\times 10^4$) | 67.21∼67.61 ms ( $\times 10^4$) |
|---|---|---|---|---|
| $y_s$ | 8.199149122 | 0.884065397 | 1.006481181 | 0.821093226 |
| | 8.193275115 | 1.237366221 | 1.222369614 | 1.1591075 |
| | 8.195800767 | 1.268553616 | 1.220610841 | 1.234773283 |
| | 8.200696404 | 1.256562369 | 1.209011696 | 1.228055312 |
| | 8.199974365 | 1.239185312 | 1.194009965 | 1.211041845 |
| | 8.203136892 | 1.224408683 | 1.178399255 | 1.196476421 |
| | 8.206666706 | 1.210725345 | 1.169886902 | 1.182864 |
| | 8.199025101 | 1.200798109 | 1.160703245 | 1.17019214 |
| | 8.200745519 | 1.193719152 | 1.152618887 | 1.163920174 |
| | 8.196222451 | 1.186434718 | 1.147769102 | 1.152477089 |
| | 8.192787658 | 1.179980846 | 1.14590337 | 1.145150522 |
| | 8.189074124 | 1.22887638 | 1.220409767 | 1.162449773 |
| | 8.189483868 | 1.265146609 | 1.255477593 | 1.241376116 |
| | 8.193790048 | 1.257261387 | 1.245696501 | 1.246065326 |
| | 8.200524923 | 1.240402637 | 1.227972468 | 1.231319681 |
| | 8.200281068 | 1.221623113 | 1.21040503 | 1.211291069 |
| | 8.204378909 | 1.211436924 | 1.200583793 | 1.195730665 |
| | 8.206938240 | 1.207789305 | 1.198157834 | 1.187584018 |
| | 8.200463269 | 1.206603078 | 1.198050721 | 1.185827676 |
| | 8.195378163 | 1.206532654 | 1.198430168 | 1.18617065 |
| | 8.198747941 | 1.202205455 | 1.19148167 | 1.184129485 |
| | 8.193689967 | 1.20800041 | 1.217585089 | 1.180466516 |
| | 8.197987606 | 1.218310845 | 1.248318944 | 1.218608922 |
| | 8.204146349 | 1.212836883 | 1.240437001 | 1.236161551 |
| | 8.201954416 | 1.205162304 | 1.227476207 | 1.228633399 |
| | 8.201796959 | 1.18633177 | 1.213584192 | 1.212538135 |
| | 8.195225700 | 1.176536791 | 1.199170172 | 1.19614337 |
| | 8.196156737 | 1.17151302 | 1.194639228 | 1.187417238 |
| | 8.201450330 | 1.166413553 | 1.192982943 | 1.179774566 |
| | 8.201550862 | 1.167595133 | 1.191167537 | 1.180549357 |
| | 8.197289073 | 1.167729574 | 1.193145369 | 1.178415334 |
| | 8.203398973 | 1.162380894 | 1.178007061 | 1.174061009 |
| Average | 8.198787113 | 1.199140265 | 1.19534198 | 1.183433293 |

eliminate the bouncing of articles problem.

### 3) What is the estimated theoretical weighing accuracy for a given conveyor belt velocity?

With a view to improving on the speed of the low-pass filter currently used, we considered two different approaches. A simple geometric approach gives very fast filtering that looks promising for removing much of the effect of oscillations at the natural frequency of the

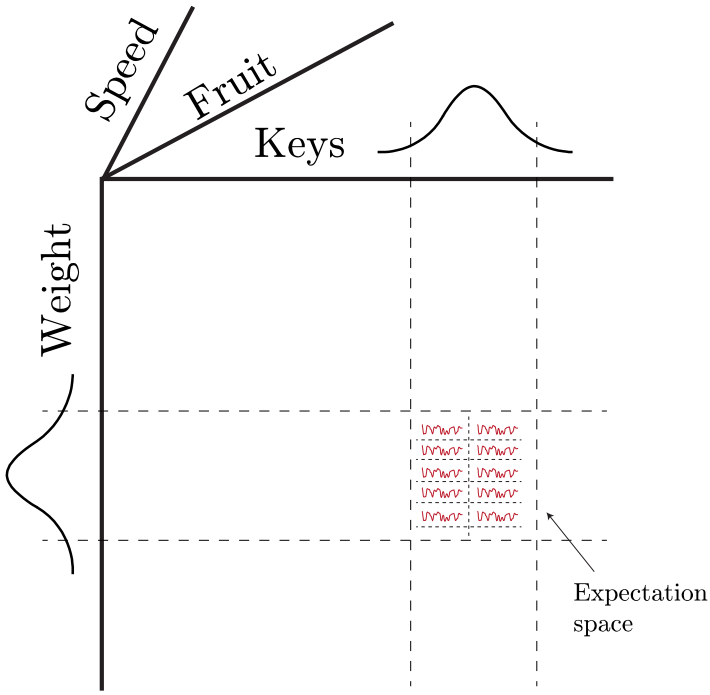


Figure 17: Decision matrix.

load and key and load-cell. We also considered a more sophisticated approach, fitting a multi-parameter damped harmonic motion solution plus a step function to successive segments of the raw signal coming from one load-cell, using the Levenberg-Marquardt method with carefully chosen initial conditions to assist convergence. The results are very promising, providing very rapid filtering of the signal as illustrated by the piecewise step-functions in Figure 16. The filtered signal (the step-functions) that is visible in this figure, when viewed over the entire time-period that a key is on the load-cell, appears to be decaying steadily. This might indicate that the window used to fit the decaying signal is too narrow, and that a wider window might give better estimates of the decay rate, resulting in filtered signals that are closer to constant and that provide a more accurate measure of weight.

# Acknowledgements

We are grateful for the support and sponsorship of Victoria University of Wellington, KiwiNet including Seumas McCroskery, ANZIAM New Zealand Branch, the Centre for Maths in Industry, the New Zealand Mathematical Society, the MINZ Directors including Professor Graeme Wake, Compac Limited for the data used, especially Andrew McIntyre and Ben Goodger from Compac, and the other team members of our international study group, including David Waters, June-Yub Lee, Masahiro Yamamoto, Xudong Liu, and Rose Davies.

# References


[1] MINZ 2004. Case Study Compac.
http://www.minz.org.nz/assets/downloads/Case-Study-Compac.pdf

[2] Kesilmis, Z., & Baran, T. (2016). *A Geometric Approach to Beam Type Load Cell Response for Fast Weighing.* Retrieved from
http://link.springer.com/article/10.1007/s12647-016-0168-2

[3] K. Levenberg. A method for the solution of certain non-linear problems in least squares. *Quarterly of applied mathematics*, 2(1944), pp. 164–168.

[4] D.W. Marquardt. An algorithm for least-squares estimation of nonlinear parameters. *Journal of the society for Industrial and Applied Mathematics*, 11(1963), pp. 431–441.


## Author addresses


1. **Stefanie Gutschmidt**, University of Canterbury, Christchurch, New Zealand.
mailto:stefanie.gutschmidt@canterbury.ac.nz

2. **Mark McGuinness**, Victoria University of Wellington, New Zealand.

3. **William Munn**, Victoria University of Wellington, New Zealand.

4. **James Hannam**, The University of Auckland, Auckland, New Zealand.

5. **Emma Greenbank**, Victoria University of Wellington, New Zealand.

6. **Soomin Jeon**, KAIST, Daejeon, 34141, Korea.

7. **Chang-Ock Lee**, KAIST, Daejeon, 34141, Korea.

8. **Celia Kueh**, Massey University, Palmerston North, New Zealand.

9. **Tony Gibb**, Adelaide Advanced Engineering, Adelaide, Australia.

10. **Ben Goodger**, Compac Sorting Equipment Ltd., Auckland, New Zealand.

11. **Andrew McIntyre**, Compac Sorting Equipment Ltd., Auckland, New Zealand.